Journal Pre-proofs

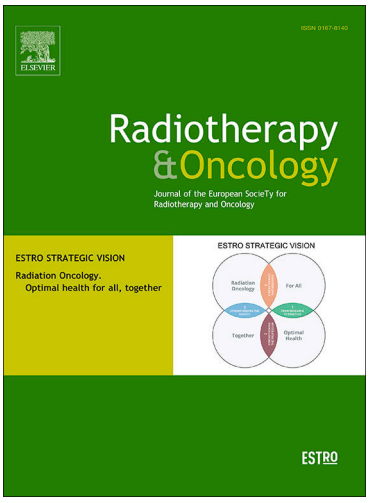

Original Article

Long-term prediction of radiation-induced optic neuropathy: A mixed-effects analysis of visual field kinetics following proton therapy

Thao-Nguyen Pham, Thibaud Mathis, Nathan Azemar, Anthony Vela, Jean-Claude Quintyn, Juliette Thariat

PII: S0167-8140(25)05209-0
DOI: https://doi.org/10.1016/j.radonc.2025.111205
Reference: RADION 111205

To appear in: *Radiotherapy and Oncology*

Received Date: 28 July 2025
Revised Date: 22 September 2025
Accepted Date: 4 October 2025

Please cite this article as: Pham, T-N., Mathis, T., Azemar, N., Vela, A., Quintyn, J-C., Thariat, J., Long-term prediction of radiation-induced optic neuropathy: A mixed-effects analysis of visual field kinetics following proton therapy, *Radiotherapy and Oncology* (2025), doi: https://doi.org/10.1016/j.radonc.2025.111205

This is a PDF file of an article that has undergone enhancements after acceptance, such as the addition of a cover page and metadata, and formatting for readability, but it is not yet the definitive version of record. This version will undergo additional copyediting, typesetting and review before it is published in its final form, but we are providing this version to give early visibility of the article. Please note that, during the production process, errors may be discovered which could affect the content, and all legal disclaimers that apply to the journal pertain.

© 2025 Published by Elsevier B.V.

Journal Pre-proofs

Long-term prediction of radiation-induced optic neuropathy: A Mixed-Effects Analysis of Visual Field Kinetics Following Proton Therapy

Thao-Nguyen Pham[1], Thibaud Mathis[2], Nathan Azemar[3], Anthony Vela[4], Jean-Claude Quintyn[5], Juliette Thariat[1,3]

[1] Department of Radiation Oncology, Centre François Baclesse, Caen, Normandy

[2] Service d'Ophtalmologie, Hôpital de La Croix-Rousse, Hospices Civils de Lyon, 69004 Lyon, France

[3] Laboratoire de physique corpusculaire UMR6534 IN2P3/ENSICAEN, Université de Caen- Normandie

[4] Medical Physics Department, Centre François Baclesse, Caen, France

[5] Department of Ophthalmology, University Hospital, Caen, Normandy

Abstract

Introduction: Radiation-induced optic neuropathy (RION) is a rare but serious complication of radiotherapy, leading to progressive vision loss. The temporal dynamics of RION are poorly understood, limiting effective monitoring and intervention. We developed a predictive mixed-effects model of visual field deterioration, a sensitive surrogate marker for clinically-reported RION, by integrating longitudinal clinical and dosimetric data, to anticipate long-term visual outcomes.

Methods: Out of a prospective database of 238 patients, 179 eyes from 105 patients treated with pencil beam scanning proton therapy were included. All selected eyes had no significant visual field deficit at baseline, defined as a mean visual sensitivity loss better than -6 dB. Baseline clinical characteristics, detailed dosimetric data, and longitudinal visual field assessments were collected. Temporal changes in mean visual sensitivity were analyzed using feature selection through random forest models and linear regression. A nonlinear mixed-effects model was then developed to predict the trajectory of visual field deterioration over time.

Results: Visual field deterioration progressed significantly over time, with a quadratic model best capturing the kinetics. Mean sensitivity loss accelerated with increasing age and clinical target volume. Incorporating the full dose-volume histogram, the volume of the optic chiasma received at least 40 Gy (V_{40}/chiasma), improved model performance. Simulation based on this model showed that the probability of RION increased sharply over time: 4.6% at 2 years, and 28.3% at 5 years.

Conclusion: This model confirms and expands upon prior work by showing that clinical factors can outweigh dosimetric ones in predicting RION progression. Our model was capable of predicting long-term visual outcomes even in patients with limited follow-up.

Keywords: radiation-induced optic neuropathy, predictive modeling, simulation, visual field deficit

Journal Pre-proofs

Journal Pre-proofs

Highlights

- RION is a delayed complication of RT, trackable via visual field sensitivity loss.
- Visual sensitivity declined over time after radiotherapy, best captured by a quadratic model.
- Older age and larger target volumes predicted faster visual field deterioration.
- Chiasma V40 (≥40 Gy) improved model performance for predicting field loss.
- Simulated risk of grade 2+ RION increased from 4.6% at 2years to 28.3% at 5years.

Journal Pre-proofs

Journal Pre-proofs

1 Introduction

Proton therapy has emerged as a highly conformal radiation modality for treating central nervous system (CNS) and head-and-neck cancers, offering precise tumor control while minimizing the volumes of adjacent healthy tissues exposed to radiation [1]. Despite its advantages, pencil beam scanning (PBS) proton therapy still poses a significant risk of late radiation-induced toxicity to critical structures, particularly the optic pathways [2]. Radiation-induced optic neuropathy (RION) is a serious late complication, as it can result in profound, irreversible visual loss. Even when modern dose constraints are respected, the incidence of clinically-significant RION is about 4%, highlighting the need for improved understanding and prevention strategies [3].

Most of the available data on RION come from retrospective studies that primarily document late, clinically evident vision loss. These studies are often limited by small sample sizes, inconsistent definitions of visual endpoints, and a lack of systematic, longitudinal ophthalmologic assessment [4,5]. Furthermore, they typically rely on visual acuity changes as the primary measure of optic nerve injury [6], despite evidence suggesting that visual field deficits may be a more sensitive and earlier indicator of optic nerve damage which is intensively studied in optic nerve disease such as glaucoma [7,8]. Several recent reports have described cases of early and progressive visual deterioration following radiotherapy, but there are currently no comprehensive models to predict the individual patient risk of early damage of the optic nerve that can lead to RION.

Visual field testing, particularly automated static perimetry, offers a sensitive method for detecting early functional impairment of the optic nerves and chiasm [9]. Changes in visual field sensitivity often precede reductions in visual acuity, providing a critical window for identifying subclinical injury before irreversible damage occurs. Tracking the kinetics of visual field deterioration over time thus represents a promising strategy for early detection of RION. However, no studies have leveraged longitudinal visual field data to model the evolution of optic pathway injury after proton therapy.

In this study, we addressed these gaps by prospectively evaluating a cohort of patients treated with PBS proton therapy, all of whom had preserved vision at baseline. Using a longitudinal mixed-effects modeling approach, we sought to characterize the kinetics of visual field decline after proton therapy, identify clinical and dosimetric predictors of accelerated deterioration, and develop a model capable of predicting long-term visual outcomes even in patients with limited follow-up.

2 Methods

2.1 Data Collection and Patient Characteristics

This prospective study included a cohort of patients treated with PBS proton therapy for CNS or head-and-neck cancers since 2018; with Institutional Review Board approval (INT-24-016). For patients at risk for optic deterioration requiring comprehensive ophthalmologic assessment at baseline, twice yearly for two years and yearly thereafter, cohort enrichment was performed by selecting patients diagnosed with tumors at risk for ocular toxicities during the weekly proton therapy tumor board meetings.

From an initial (2018-2023) cohort of 238 patients, 105 patients were included based on the availability of baseline and longitudinal visual field perimetry data, with exclusion of those who had significant baseline visual loss, defined as a mean visual field deficit lower than -6 dB (In glaucoma, this 6-decibel deficit allows for classification of minimal to moderate impairment [10]). Patients with early major deficits or with inconsistent ophthalmologic data were excluded to ensure uniformity of baseline visual status and avoid modeling potential recovery. Institutional Review Board (IRB) approval was obtained, and all patients provided informed consent.

Visual field perimetry was chosen detection of subclinical RION. Visual field testing was conducted using automated static perimetry (Metrovision Field 30), measuring differential light sensitivities at multiple fixed points. Global indices such as the visual field mean deficit were calculated and used for analysis. Standardized ophthalmological evaluations were scheduled at baseline, and then at regular intervals post-treatment, with details provided in the study protocol. RION was assessed using a visual field-based grading system adapted

Journal Pre-proofs
from glaucoma studies [11] since visual acuity alone often underestimates early optic neuropathy, given that central macular function may remain intact until late in the disease course. The visual field–based grading therefore provides a more sensitive and specific method of capturing optic nerve injury. Visual toxicity was classified in 3 dB increments: grade 0 (0 to –3 dB), grade 1 (–3 to –6 dB), grade 2 (–6 to –9 dB), grade 3 (–9 to –12 dB), and grade 4 (<–12 dB).

For the purposes of this study, "toxicity" refers to the occurrence of Grade ≥1 RION, i.e., a mean visual field deficit exceeding –3 dB relative to baseline.

Tumor and organ-at-risk (OAR) delineation were performed using high-resolution millimetric computed tomography (CT) scans and the RayStation Treatment Planning System (RaySearch®). Among optic organs, we focused on the optic nerves, the chiasma, as well as the retina, the ganglion cell layer constituting the head; i.e. the axons, of the optic nerve in the retina. Dose calculations were conducted using a Monte Carlo algorithm and accounted for a relative biological effectiveness (RBE) factor of 1.1. Treatment was delivered with the IBA ProteusONE system using PBS proton therapy.

Current understanding of RION suggests involvement of the optic nerve and chiasma, defined by a serial architecture, which is expressed in treatment plans as maximal doses, or doses to small volumes (such as 1%, 2%, 0.01cc) of the organ. It should be noted that these metrics are systematically applied as clinical goals during the definition of objectives of the inverse planning phase. The maximal dose to the optic nerve and chiasma was generally capped below 52.2 Gy (with exceptions when one of the eyes had to be sacrificed due to tumor location) in recent clinical studies. Therefore, other metrics on the DVH may be needed to further reduce the risk of RION. Full DVH were available including dose distribution metrics reported as the percent dose received by 1, 2, 5, 10, 20, … 90, 95, 98% of the volumes (D1, D2, D5, D10–D90, D95, D98). The minimum dose (Dmin), mean dose (Dmean), and maximum dose (Dmax) and volume metrics receiving 1, 5, 10, 20, 30, 40, 50, and 60 Gy. In total, there were 67 dosimetric parameters (including the total radiation dose) for each eye of each patient.

Clinical data collected included demographic information such as age and sex, as well as metabolic/vascular conditions including hypertension, hypercholesterolemia, and diabetes. Smoking history was documented as a potential risk factor. Treatment-related factors were recorded, including the number of surgeries, concomitant chemotherapy, and tumor control status (stable disease, partial response, complete response versus progressive disease or recurrence). Distances from the clinical target volume (CTV) and optic OARs were also calculated. Baseline visual function, before proton therapy, was systematically collected.

2.2 Longitudinal analysis of visual field deficit after radiotherapy

To evaluate the long-term impact of radiotherapy on visual field deterioration, we developed a structured longitudinal modeling approach. Two models were evaluated including (1) Model considering dosimetric (Dmin, Dmean, Dmax) parameters, and (2) Model considering the full DVHs.

The first step involved characterizing the relationship between time elapsed since radiotherapy and visual field mean deficit. Correlation analysis and random forest modeling were used to determine the significance of time as a predictive variable. We then compared several candidate model structures to describe the temporal evolution of VF deficits, including linear, quadratic, and cubic models. Each model treated visual field deficit as a function of time post-radiotherapy. Model performance was evaluated using Akaike Information Criterion (AIC), Bayesian Information Criterion (BIC), and root mean squared error (RMSE).

The next phase focused on identifying relevant clinical and dosimetric predictors associated with visual field mean deficit decline. We first removed variables with high intercorrelation (Pearson's $R > 0.8$) to avoid multicollinearity. A random forest model was then employed to identify features with the highest importance in predicting changes in visual field mean deficit. Variable importance was quantified by the percentage increase in mean squared error (%IncMSE) when each variable was permuted. Variables with the highest %IncMSE values were considered to have high importance. The most influential variables from this process were incorporated into the longitudinal model. To account for inter-subject and inter-eye variability, we used a mixed-effects

Journal Pre-proofs

modeling framework. The selected features from the random forest analysis were introduced into the model through a forward stepwise selection process. Forward stepwise selection was performed by sequentially adding candidate predictors identified by random forest analysis. At each step, inclusion was determined by improvement in model fit using likelihood ratio tests, AIC, and BIC. This process continued until no further significant improvement was achieved. With the final mixed-effects model established, we simulated the long-term trajectory of VF deficits over a 10-year period following radiotherapy for each eye.

With the final mixed-effects model established, we simulated the long-term trajectory of VF deficits over a 10-year period following radiotherapy for each eye. To be noted, these simulations should be interpreted as mathematical extrapolations rather than direct clinical observations.

Time-to-event curves were generated using the final models to predict the development of visual toxicity under different clinical and dosimetric conditions. The general workflow was illustrated on Figure 1.

3 Results

A statistically significant negative correlation was observed between post-radiotherapy visual field mean deficit (relative to baseline) and time since treatment (R=-0.26, $p < 0.001$, Figure 2A). At the population level, visual function demonstrated a progressive decline over time, with linear regression analysis estimating a mean annual reduction of 0.63 dB. Although this general trend indicated a deterioration in visual performance, substantial inter-individual variability was noted.

Among the 179 eyes, there were 70 patients (100 eyes) who received a maximal dose ≤ 52.2 Gy, while 50 patients (79 eyes) exceeded this threshold. The incidence of toxicity was 18% (18/100 eyes) in the ≤ 52.2 Gy group and 30% (24/79 eyes) in the > 52.2 Gy group (Table S1). In the ≤ 52.2 Gy group, MD declined by –0.55 units per time point (95% CI, –0.78 to –0.32; $p < 0.001$), while in the > 52.2 Gy group there was an additional decline of –0.36 units per time point (95% CI, –0.74 to 0.02; $p = 0.058$), corresponding to an overall slope of –0.92 units per time point. Baseline MD values did not differ significantly between dose groups ($p = 0.55$) (Table S2, Figure S1).

Feature selection via random forest modeling identified elapsed time since radiotherapy as the most predictive variable for visual field mean deficit reduction rate, followed by patient age and radiation dose metrics involving the optic apparatus, particularly the optic chiasm and optic nerves (Figure 2B).

To characterize the trajectory of visual deterioration, several time-based models were assessed. A quadratic model best represented the relationship between visual field mean deficit change and time after radiotherapy, outperforming both linear and cubic models (Table 2). Model selection was based on AIC = 5431.7, BIC = 5467.0, and RMSE = 1.777, indicating a non-linear decline in visual field mean deficit sensitivity.

A multivariate model incorporating dosimetric (Dmin, Dmean, Dmax) and clinical parameters was refined through stepwise selection and assessment of multicollinearity (Figure S1). The final predictors included concomitant chemotherapy, gender, diabetes, hypertension, cholesterolemia, smoking, CTV, total radiation dose, maximum dose to the retina, maximum dose to the optic nerve, mean and maximum dose to the chiasma, baseline visual field deficit, and tumor progression. The stepwise-selected model included time after radiotherapy, age, CTV, mean dose to the chiasma, and maximum dose to the optic nerve. This model yielded improved performance (AIC = 2836.2; BIC = 2899.1; RMSE = 1.28).

Mixed-effects modeling demonstrated a significant negative association between mean dose to the chiasma and visual field sensitivity ($p = 0.01$). Furthermore, interaction effects involving time, age, and CTV were statistically significant. Parameter estimation was presented in Table S3.

$$\Delta MD \sim \beta_1 \cdot Time_{after_{RT}} \cdot (Age + CTV) + \beta_2 \cdot Time_{after_{RT}}{}^2 + \beta_3 \cdot Dmean_{chiasma} + (1 + Time_{after_{RT}} | ID)$$

Where ΔMD is the change in mean deficit of visual field perimetry at a given time after radiotherapy, measured in decibels (dB). $Time_{after_{RT}}$ is the time since radiotherapy, measured in years. Age is the age of the patient at

Journal Pre-proofs

the time of radiotherapy, measured in years, and CTV is the clinical target volume for radiotherapy, measured in cubic centimeters (cm³). $Dmean_{chiasma}$ is the mean radiation dose delivered to the optic chiasma, measured in Gray (Gy). ID represents the patient identifier, used as a grouping factor for random effects. The coefficients β represent the effects of the corresponding predictors. Specifically, β_1 (dB per (year × (year + cm³))) captures the effect of the interaction between time after radiotherapy and the combined influence of age and CTV on ΔMD. β_2 (dB per month²) captures the effect of the quadratic term of time after radiotherapy. β_3 (dB per Gy) represents the effect of the mean dose to the optic chiasma on ΔMD. The random effects term $1 + Time_{after_{RT}} | ID$ allows each patient to have their own baseline visual field deficit (intercept) and an individual slope of change over time, accounting for repeated measures within patients.

In this model, Dmean to the chiasma was included as a main effect but not as an interaction term with time. Consistent with Figure 3, Dmean exhibited limited impact on visual sensitivity compared with age, CTV, and V40 of the chiasma. Using this model, predicted times to developing Grade ≥1 RION were stratified by age and CTV (Figure 2, Table 3). The proportion of patients without visual toxicity, i.e. RION by VF at 2, 5, and 10 years post-treatment was 95.4%, 71.7%, and 0.8%, respectively. Greater CTV volumes were significantly associated with earlier onset of visual toxicity (Figure 3, Table 3). To be noted, predictions at 10 years should be interpreted with caution, as they are based on extrapolation with limited patient numbers at risk and thus represent exploratory estimates rather than definitive outcomes.

An extended model incorporating DVH parameters was developed. Random forest analysis highlighted the following as key predictors: age, volume of chiasma receiving ≥40 Gy (V_{40} chiasma), and distances from CTV to both the optic nerve and retina (Figure S2). The selected model from stepwise covariate selection included time after radiotherapy, age, and V40_chiasma, along with quadratic and interaction terms, yielding improved performance metrics (AIC = 2172.7, BIC = 2228.5, RMSE = 1.03). Parameter estimation was presented in Table S3.

$$\Delta MD \sim \beta_1 . Time_{after_{RT}} . (Age + V_{40chiasma}) + \beta_2 . Time_{after_{RT}}{}^2 . (Age + V_{40chiasma}) + (1 + Time_{after_{RT}} | ID)$$

Where ΔMD is the change in mean deficit of visual field perimetry at a given time after radiotherapy, measured in decibels (dB). $Time_{after_{RT}}$ is the time since radiotherapy, measured in years. Age is the age of the patient at the time of radiotherapy, measured in years, and $V_{40chiasma}$ is The volume of the optic chiasma (in cubic millimeters or cm³) that received at least 40 Gy of radiation. ID represents the patient identifier, used as a grouping factor for random effects. The coefficients β represent the effects of the corresponding predictors. Specifically, β_1 (dB per (year × (year + % volume))) captures Effect of the interaction between time after radiotherapy and the combined influence of age and V40_chiasma on ΔMD. β_2 (dB per year²·(year + volume)) captures effect of the quadratic time term interacting with the combined influence of age and V40_chiasma. The random effects term $1 + Time_{after_{RT}} | ID$ allows each patient to have their own baseline visual field deficit (intercept) and an individual slope of change over time, accounting for repeated measures within patients.

Using this model, predicted time to toxicity progression revealed that patients with a V_{40} chiasma greater than 75% had a shorter time to develop higher grades of toxicity compared to those with a lower V_{40} chiasma exposure (Figure 3, Table 3).

A strong correlation (R^2 = 0.86) was observed between V_{40} chiasma, mean dose to the chiasma, and CTV, suggesting that exposure of chiasma mediated the effects of tumor size and dose distribution on visual field outcomes. Tumor positioning metrics were predictive of mean dose to the chiasma (Figure 3).

4 Discussion

This study provides a comprehensive longitudinal analysis of visual field deterioration following proton therapy in patients with paraoptic tumors. Using visual field perimetry to follow the progression of RION, we found a statistically significant and progressive decline in visual field mean deficit over time. Our findings suggest that RION evolves along a non-linear trajectory, influenced by both dosimetric and clinical factors, with important implications for long-term patient monitoring.

Journal Pre-proofs

Our findings demonstrate that radiotherapy contributes to a progressive decline in visual function over time, with the trajectory of deterioration most accurately represented by a quadratic model. Prior studies have described the delayed onset and insidious progression of RION, particularly in patients receiving high doses to the anterior visual pathway [12]. However, current Normal Tissue Complication Probability (NTCP) models primarily focus on predicting the incidence of RION, without addressing *when* toxicity develops [3,13–16]. This temporal limitation reduces their clinical utility, especially in long-term survivors where toxicity may not manifest until several years post-treatment. Moreover, most existing NTCP models are derived from cohorts with relatively short follow-up periods and a predominance of malignant cases, which inherently limits their ability to capture delayed toxicities in patients with benign tumors. These patients often have prolonged survival, increasing their risk of developing late-onset complications that go undetected in shorter studies [17]. Our model was capable of estimating long-term trajectories of visual decline, even in patients with limited follow-up, by leveraging population-level longitudinal information. The valid timeframe for prediction is restricted to the observed follow-up period in our cohort of 5 years. Predictions at 10 years should be interpreted with caution, as they are based on extrapolation with limited patient numbers at risk and thus represent exploratory estimates rather than definitive outcomes.

Our study identified key predictors of individual variability in visual decline, including age, tumor volume, and radiation dose/volume to the chiasma. Notably, older patients exhibited a faster rate of decline, likely due to age-associated reductions in neural repair mechanisms and heightened vulnerability to oxidative stress and mitochondrial dysfunction under ionizing radiation exposure [18]. Larger tumor volumes may also necessitate higher doses or broader radiation fields, increasing optic pathway exposure and risk. Noticeably, we found that a dose–volume histogram-based model—incorporating volumetric radiation exposure to the optic pathway—outperformed traditional models that rely solely on point-based dosimetric parameters such as maximum dose or mean dose. This supports earlier work for the inclusion of spatial dose distribution in NTCP modeling to improve its predictive accuracy [19]. Dose to the chiasma was lower than in previous models. The improved performance of DVH-based models in our study highlights the value of integrating detailed anatomic and dose-volume information when assessing the risk of radiation-induced visual decline. These findings also align with the growing emergence of *dosiomics*, an advanced approach that leverages high-dimensional dosimetric features to capture complex spatial dose patterns and further enhance model performance [20].

Several limitations should be acknowledged in this study. First, a longer follow-up period would be beneficial to better assess long-term toxicity, which is particularly important for predicting patients with benign tumor. The model predictions after 5 years should be considered with caution. Additionally, the sample size could be larger to enhance the statistical power and generalizability of the findings. The considerable inter-individual variability observed may be better captured by using more specific mechanistic endpoints, as RION can result from various mechanisms, such as vascular damage or myelin degeneration [21,22] or individual radiosensitivity. Furthermore, patients with pre-existing optic nerve damage before radiotherapy were not included in the study, which may limit the applicability of the results to this subgroup of patients.

The result of this study highlights the potential to improve proton therapy planning by incorporating volumetric dose constraints—particularly limiting the volume of the optic chiasma receiving high radiation doses—to better predict and reduce the risk of radiation-induced visual field loss. The development of individualized, time-based risk models also offers a promising tool for tailoring patient counseling and follow-up. In practice, by specifying patient age, dosimetric parameters, and follow-up time, our model can generate individualized risk estimates of visual field decline. This has two main applications: (1) treatment planning—allowing optimization of plans to minimize predicted long-term toxicity; and (2) clinical follow-up—guiding the intensity and timing of ophthalmologic monitoring based on individualized risk, thereby facilitating early intervention when indicated. However, before widespread clinical adoption, these approaches require validation in larger, diverse populations and integration into existing workflows, which will demand close collaboration between radiation oncologists, dosimetrists, and ophthalmologists. Additionally, expanding assessment beyond visual field testing to include broader functional and quality-of-life measures is needed to fully translate these insights into routine practice.

5 Conclusion

Our model effectively predicts RION by analyzing longitudinal visual field changes in relation to both clinical and dosimetric parameters. While incorporating DVH-based dosimetric data improved model performance, clinical variables such as age and tumor volume were equally or more influential in predicting visual decline. These findings support individualized radiotherapy strategies that integrate both clinical and dosimetric risk factors to minimize optic nerve damage.

Funding

Funding includes PMRT ERDF-FSE 2014-2020 (Grant No. 18P03532/18 E01765), SEQ-RTH22 (Subvention No. 2023-017 from INCa) for voxel-based analysis of toxicities, and the PTCOG Research Grant 2024 for Medicine.

Author contribution statement

TNP and JT contributed to conceptualization. TNP carried out modeling, data analysis, and manuscript writing. NA was responsible for data management. TNP, TM, and JT contributed to the interpretation of results. All authors reviewed and approved the final version of the manuscript.

Conflicts of interest

All remaining authors have declared no conflicts of interest.

References

[1] K. Bała, Y. Samovich, K. Dorobisz, Proton Therapy in The Treatment of Head And Neck Cancers- Review, Curr Oncol Rep 26 (2024) 1380–1387. https://doi.org/10.1007/s11912-024-01592-9.

[2] M. Kountouri, A. Pica, M. Walser, F. Albertini, A. Bolsi, U. Kliebsch, B. Bachtiary, C. Combescure, A.J. Lomax, R. Schneider, D.C. Weber, Radiation-induced optic neuropathy after pencil beam scanning proton therapy for skull-base and head and neck tumours, Br J Radiol 93 (2020) 20190028. https://doi.org/10.1259/bjr.20190028.

[3] A. Köthe, P. Van Luijk, S. Safai, M. Kountouri, A.J. Lomax, D.C. Weber, G. Fattori, Combining Clinical and Dosimetric Features in a PBS Proton Therapy Cohort to Develop a NTCP Model for Radiation-Induced Optic Neuropathy, International Journal of Radiation Oncology*Biology*Physics 110 (2021) 587–595. https://doi.org/10.1016/j.ijrobp.2020.12.052.

[4] F.G. Ataídes, S.F.B.R. Silva, J.J.C.M.D.C. Baldin, Radiation-Induced Optic Neuropathy: Literature Review, Neuroophthalmology 45 (2021) 172–180. https://doi.org/10.1080/01658107.2020.1817946.

[5] A.R. Carey, B.R. Page, N. Miller, Radiation-induced optic neuropathy: a review, Br J Ophthalmol 107 (2023) 743–749. https://doi.org/10.1136/bjo-2022-322854.

[6] U.S. Department of Health and Human Services, National Institutes of Health, National Cancer Institute, Common Terminology Criteria for Adverse Events (CTCAE) Version 5.0, U.S. Department of Health and Human Services, Bethesda, MD, 2017. https://ctep.cancer.gov/protocoldevelopment/electronic_applications/ctc.htm.

[7] A. Bayer, P. Harasymowycz, J.D. Henderer, W.G. Steinmann, G.L. Spaeth, Validity of a new disk grading scale for estimating glaucomatous damage: correlation with visual field damage, American Journal of Ophthalmology 133 (2002) 758–763. https://doi.org/10.1016/S0002-9394(02)01422-8.

[8] U. Guthauser, J. Flammer, P. Niesel, The relationship between the visual field and the optic nerve head in glaucomas, Graefe's Arch Clin Exp Ophthalmol 225 (1987) 129–132. https://doi.org/10.1007/BF02160344.

Journal Pre-proofs

[9] S. Kedar, D. Ghate, W.F. Corbett, Visual fields in neuro-ophthalmology, Indian J Ophthalmol 59 (2011) 103–109. https://doi.org/10.4103/0301-4738.77013.

[10] A.A. Jammal, N.G. Ogata, F.B. Daga, R.Y. Abe, V.P. Costa, F.A. Medeiros, What Is the Amount of Visual Field Loss Associated With Disability in Glaucoma?, Am J Ophthalmol 197 (2019) 45–52. https://doi.org/10.1016/j.ajo.2018.09.002.

[11] Advanced Glaucoma Intervention Study. 2. Visual field test scoring and reliability, Ophthalmology 101 (1994) 1445–1455.

[12] Z. Zhao, Y. Lan, S. Bai, J. Shen, S. Xiao, R. Lv, B. Zhang, E. Tao, J. Liu, Late-onset radiation-induced optic neuropathy after radiotherapy for nasopharyngeal carcinoma, Journal of Clinical Neuroscience 20 (2013) 702–706. https://doi.org/10.1016/j.jocn.2012.05.034.

[13] C. Mayo, M.K. Martel, L.B. Marks, J. Flickinger, J. Nam, J. Kirkpatrick, Radiation Dose–Volume Effects of Optic Nerves and Chiasm, International Journal of Radiation Oncology*Biology*Physics 76 (2010) S28–S35. https://doi.org/10.1016/j.ijrobp.2009.07.1753.

[14] V. Moiseenko, W.Y. Song, L.K. Mell, N. Bhandare, A comparison of dose-response characteristics of four NTCP models using outcomes of radiation-induced optic neuropathy and retinopathy, Radiat Oncol 6 (2011) 61. https://doi.org/10.1186/1748-717X-6-61.

[15] Y.-L. Wu, W.-F. Li, K.-B. Yang, L. Chen, J.-R. Shi, F.-P. Chen, X.-D. Huang, L. Lin, X.-M. Zhang, J. Li, Y.-P. Chen, L.-L. Tang, Y.-P. Mao, J. Ma, Long-Term Evaluation and Normal Tissue Complication Probability (NTCP) Models for Predicting Radiation-Induced Optic Neuropathy after Intensity-Modulated Radiation Therapy (IMRT) for Nasopharyngeal Carcinoma: A Large Retrospective Study in China, Journal of Oncology 2022 (2022) 1–10. https://doi.org/10.1155/2022/3647462.

[16] E.R. Nafchi, P. Fadavi, S. Amiri, S. Cheraghi, M. Garousi, M. Nabavi, I. Daneshi, M. Gomar, M. Molaie, A. Nouraeinejad, Radiomics model based on computed tomography images for prediction of radiation-induced optic neuropathy following radiotherapy of brain and head and neck tumors, Heliyon 11 (2025) e41409. https://doi.org/10.1016/j.heliyon.2024.e41409.

[17] A. Dutz, A. Lühr, E.G.C. Troost, L. Agolli, R. Bütof, C. Valentini, M. Baumann, X. Vermeren, D. Geismar, B. Timmermann, M. Krause, S. Löck, Identification of patient benefit from proton beam therapy in brain tumour patients based on dosimetric and NTCP analyses, Radiotherapy and Oncology 160 (2021) 69–77. https://doi.org/10.1016/j.radonc.2021.04.008.

[18] J. Tong, T.K. Hei, Aging and age-related health effects of ionizing radiation, Radiation Medicine and Protection 1 (2020) 15–23. https://doi.org/10.1016/j.radmp.2020.01.005.

[19] M.A. Ebert, S. Gulliford, O. Acosta, R. De Crevoisier, T. McNutt, W.D. Heemsbergen, M. Witte, G. Palma, T. Rancati, C. Fiorino, Spatial descriptions of radiotherapy dose: normal tissue complication models and statistical associations, Phys. Med. Biol. 66 (2021) 12TR01. https://doi.org/10.1088/1361-6560/ac0681.

[20] B. Liang, H. Yan, Y. Tian, X. Chen, L. Yan, T. Zhang, Z. Zhou, L. Wang, J. Dai, Dosiomics: Extracting 3D Spatial Features From Dose Distribution to Predict Incidence of Radiation Pneumonitis, Front. Oncol. 9 (2019) 269. https://doi.org/10.3389/fonc.2019.00269.

[21] S.M. Fan, W. Chen, L. Xiong, Y. Xia, Y.B. Xie, J. Chen, Magnetic resonance diffusion tensor imaging study of rhesus optic nerve radiation injury caused by a single dose/fractionation scheme stereotactic radiosurgery at an early stage, Journal of Neuroradiology 43 (2016) 207–213. https://doi.org/10.1016/j.neurad.2015.10.003.

Journal Pre-proofs

[22] Y. Wang, J. Fu, H. Zhou, H. Li, Q. Xu, J. Wei, Clinical characteristics of radiation-induced optic neuropathy: A single-center retrospective study, Advances in Ophthalmology Practice and Research 3 (2023) 141–146. https://doi.org/10.1016/j.aopr.2023.05.003.

Journal Pre-proofs

Journal Pre-proofs

Figure captions

Figure 1. Schematic of the modeling workflow

Figure 2. Temporal effect visual field deficit after radiotherapy. (A) Random forest feature selection showing predictive importance of variables. (B) Correlation between visual field mean deficit and time since treatment.

Legend: MSE: Mean square error. The blue line in panel B represents the fitted average decline in mean deficit of visual field perimetry over time. NO refers to the optic nerves.

Figure 3. Time-to-event curves predicting visual field deterioration under different clinical and dosimetric conditions

Legend: The NTCP curve depicts the average population-level risk of RION progression as a function of time post-radiotherapy, with age and dosimetric parameters set to cohort averages. Histograms illustrate simulated time-to-event distributions for different clinical and dosimetric strata. The accompanying histograms illustrate model-simulated time-to-event distributions for different clinical and dosimetric strata. These simulations should be interpreted as extrapolations from the mixed-effects model rather than direct clinical observations. The apparent convergence toward higher RION grades at later time points reflects mathematical projection beyond the median follow-up of our cohort and does not indicate inevitable severe toxicity for all patients. Importantly, these 10-year projections are derived from prospective visual field testing, a more sensitive modality than consultation-based visual acuity reporting used in prior series.

Figure 4. Final model linking the chiasma volume receiving at least 40 Gy with mean dose to the chiasma and CTV to the kinetic of visual field deficit after radiotherapy

Table captions

Table 1. Patients and treatment characteristics

Table 2. Model structure selection for visual field deficit kinetic after radiotherapy

Table 3. Time to RION estimation in relationship with dosimetric and clinical parameters

Supplementary description

Table S1. Visual field deficit according to maximum dose to optic nerve/optic chiasm: Toxicity by maximum dose to ON/OC

Table S2. Visual field deficit according to maximum dose to optic nerve/optic chiasm: GEE model estimates for MD progression

Figure S1. Observed MD trajectories (thin lines) and model-predicted mean trajectories with 95% CI (bold lines with shaded bands) according to maximum dose to ON/OC (≤ 52.2 Gy vs. > 52.2 Gy).

Figure S2. Correlation between parameters after imputation and feature importance ranking in model 2

Figure S3. Correlation between parameters after imputation and feature importance ranking in model 3

Table S3. Parameter estimation for the mixed-effect models